© 2018 IJSRSET | Volume 4 | Issue 1 | Print ISSN: 2395-1990 | Online ISSN : 2394-4099
Themed Section : Engineering and Technology

Arima Analysis for Detecting FTIR and XRD Spectral Pattern on Barium Strosium Titanat (BST) Thin Film

Muhammad Nur Aidi[1], Irzaman[2]

[1]Statistics Department, Bogor Agricultural University, Dramaga Bogor Indonesia

[2]Physics Department, Bogor Agricultural University, Kampus IPB Dramaga Bogor Indonesia

ABSTRACT

Knowledge about atomic and molecular structure of Barium Stronsium Titanat (BST) is very important for exploring the material characteristic of BST. Analyzing X-ray Diffraction and Fourier-transform Infrared (FTIR) Spectroscopy spectral pattern usually done by Rietvel model or General Structure Analysis System (GSAS). Both of these methods rely on reference pattern as guidance. XRD or FTIR data were first compared with reference data which then its charateristic indentified based on the reference data. ARIMA model could be used as alternative. ARIMA model does not need reference pattern as guidance. Research shows those FTIR and XRD values at heated BST powder could be modeled well by ARIMA. Therefore, studying atomic and molecular structure of BST could be done via reflectant function which derived from XRD and FTIR values with ARIMA approach. Result showed that first differencing model in ARIMA with order AR (2) and order MA (2) or less were very good for explaining Lanthanum Oxide (0%, 5%, and 10%) doped BST FTIR data. First differencing model in ARIMA with order AR (3), and order MA (3) or less were very good for explaining Lanthanum Oxide (0%, 5%, and 10%) doped BST XRD data. Accuracy of ARIMA model for explaining Lanthanum Oxide (0%, 5%, and 10%) doped BST FTIR data is more accurate than Lanthanum Oxide (0%, 5%, and 10%) doped BST XRD data. This is due to model ARIMA for Lanthanum Oxide (0%, 5%, and 10%) doped BST FTIR data is more simple (more parsimony) and its Determinant coefficient is higher.

Keywords: ARIMA, FTIR, XRD, BST, Lanthanum oxide

I. INTRODUCTION

In the past few years, ferroelectric material, Barium Stronsium ($Ba_{1-x}Sr_xTiO_3$, BST), has attracting attention as a chemically stable, high permitivity, high tunability and efficient ferroelectric material [1-3]. BST has varies electronic application as multilayer capacitor, Dynamic Random Access Memory (DRAM), micro wave phase, oscilator, uncooled infrared sensor, etc because of its high dielectric constant, nonlinear varied dielectric constant with electrical field, ferroelectric, piroelectric behavior, and so on. The mentioned characterisic depends on the main ingredient composition and charateristic [4-5].

Ferroelectric material had been studied extensively in form of thin film, especially as multilayer ceramic capacitor (MLCC) and dynamic random access memory (DRAM) [6]. Among many type of ferroelectric material, barium strontium titanate had been the most intensively investigated becaused of its high dielectric constant, low dielectrical loss, and good thermal stability. Other than that, its temperature range, in which its feroelectric characteristic shows, could be simply controlled by adjusting its barium-strontium ratio [7].

BST powder and thin film usually made by solid-state reaction, and hidrothermal method [8-10]. Several inovative approach, such as sprayed pyrolysis, synthetic combution, co-chemical precipitation, pulsed laser deposition (PLD), chemical vapor deposition (CVD), electrochemical, sprayed electrostatic vapor deposition, had been used to synthesize the BST powder [11-12]. BST characteristic was closely related to the composition, its mineral structure, and its molecular shape. Thus, BST detection is crucial to understand the material characteristic deeper. There are several BST detection method such as X-ray powder diffraction (XRD), and also Fourier-transform infrared spectroscopy (FTIR).

X-ray powder diffraction (XRD) is a fast analysis method that mainly used for identificating crystal material phase and retrieving information about individual cell dimension. Analyzed material is homogenysis and composition. X-ray diffraction was based on constructive disturbance of monochromatic X-ray and crystal sample [13]. X-ray was emitted by catoda ray tube, filtered to creat monochromatic radiation, collimated for concentrating, and aimed at the sample [14-16]. Interaction between the X-ray and the sample create constructive interference (and the ray diffracted) if the condition meets the Bragg Law ($n\lambda = 2d \sin \theta$). The law explain the correlation between electromagnetic radiation wavelength with diffraction angle and grid distance on the cystal sample [17]. Diffracted X-ray is then detected, proceed and calculated. By scanning the sample with range of 20 angles, all possible direction grid diffraction should be achieved due to the random orientation of the powder material. Conversion diffraction peak to distance-d enables the identification of mineral since each mineral has its unique set of distance-d. Usually, this is achieved by ratio of distance d and the standard benchmark pattern [18].

Fourier-transform infrared spectroscopy is a method used for retrieving infared spectrum in absorbtion or emission of solid-gas, solid or gas which was identified by vibration movement. Molecular vibration was unique for each molecul and usually called finger print vibration. Molecular vibration could be splitted into two groups; stretching vibration and bendig vibration. A FTIR spectrometer could simultaniously collect high resolution spectrum data through wide spectrum range. In infrared spectroscopy, infrared spectrum was in the wavelength range from 0.75 to 1000 μm or wavenumber ranges from 1300 to 1 cm^{-1}. From the application and instrumentation point of view, infrared spectrum divided into three radiation type which are near infrared (wavenumber of 12800-4000 cm^{-1}), mid infrared (wavenumber 4000-200 cm^{-1}), and far infrared (wavenumer of 200-10 cm^{-1}). This gives significant advantages over dispersive spectrometer which measure the intensity on the narrow range of wavelength over period of time. Name of Fourier-transform infrared spectroscopy comes from the fact that Fourire transformation (mathematical process) was needed to change raw data into the actual spectrum [19-21].

From the aforementioned explaination, studying atomic and molecular structure of BST are very important in order to studying the BST character itself. Analyzing X-ray Diffracton spectrum and Fourier-transform infrared spectroscopy data usually with Rietveld model or General Structure Analysis System (GSAS). Both methods are based on reference as benchmark. XRD and FTIR data are compared with the reference data which then identified its characteristics. ARIMA model could be used as alternative. ARIMA model does not need any reference pattern as benchmark. The research result showed that XRD value on the heated BST powder could be modelled well by ARIMA [56]. Thus, BST study through atomic and molecular structure could be studied through reflectant function which generated from XRD [22-39] and FTIR [40-54] value with ARIMA approach.

II. RESEARCH OBJECTIVES

1. Obtain BST ARIMA function from XRD and FTIR data,

2. Compared BST ARIMA function with Lanthanum Oksida (0 %, 5 % dan 10 %) doped BST XRD and FTIR data.

III. RESEARCH METHODOLOGY

FTIR spectrum characterization from BST thin film used FTIR tools type ABB MB 3000. In this research, FTIR spectrum used belongs to the mid infared radiaton category (wavenumber of 4000-500 cm^{-1}) with step of 16 cm^{-1}. In the Rietvel model, x axis is infrared radiation category and y axis is percent of absorption. In the ARIMA model, infrared radiation category (x axis) be changed to integer number with starting number 1 as x axis and and y axis is still percent of absorption. XRD spectrum characterization used the XRD tools type GBC EMMA. In this research XRD spectrum used belongs to angle range of 10^0 to 80^0 with step of 0.02^0 [55-58]. In the Rietvel model, x axis is X-Ray spectrum, and y axis is percent of diffraction. In the ARIMA model, X-Ray spectrum be changed to integer number with starting number 1 as as x axis and and y axis is still percent of diffraction.

ARIMA model is a model of y_t function of y_{t-1}, y_{t-2}, up to y_{t-p} and e_t, e_{t-1}, $e_{t-2,...,}$ e_{t-q} . That model can be wrote by

$$y_t = c + \emptyset_1 y_{t-1} + \emptyset_2 y_{t-2} + \cdots . + \emptyset_p y_{t-p} + \theta_1 e_{t-1} + \theta_2 e_{t-2} + \cdots + \theta_q e_{t-q} + e_t$$

$$y_t - \emptyset_1 y_{t-1} - \emptyset_2 y_{t-2} - \cdots . - \emptyset_p y_{t-p} = c + \theta_1 e_{t-1} + \theta_2 e_{t-2} + \cdots + \theta_q e_{t-q} + e_t$$

If $By_t = y_{t-1}$, $B(By_t) = B^2 y_t = y_{t-2}$ ...son.

Then

$$(1 - \emptyset_1 B - \emptyset_2 B^2 - \cdots - \emptyset_2 B^p) y_t = (1 + \theta_1 B + \theta_2 B^2 + \cdots + \theta_q B^q) e_t + c$$

The above model is ARMA (p,q) with assume y_t has stationer in average and variance. If data is not stationer in average, data to differencing between lag. y'_t is the differenced series. That a first difference is represented by $(1-B)$. Similarly, if second-order differences have to be computed, then: $y''_t = y_t - 2y_{t-1} + y_{t-2} = (1-2B+B^2)y_t = (1-B)^2 y_t$. In general, a d th-order difference can be written as $(1-B)^d y_t$. Then equation can be written as

$$(1-\phi_1 B - \cdots - \phi_p B^p)(1-B)^d y_t = c + (1+\theta_1 B + \cdots + \theta_q B^q) e_t$$

ARIMA model exploration for FTIR and XRD data were done by Box and Jenkin procedure [67]. Initial step was done to identify the data was stationary or not in mean and in variance. If it was not stationary in mean then differencing need to be done, and transformation needs to be done if it was not stationary in variance. If the data was stationary, then ACF (Autocorrelation Function) plot and PACF (Partial Autocorrelation Function) plot were done to get possible assumption model. Next step was to get estimated parameter model and to test the parameter to the models until significant model parameters were obtained. Selected model was then calculated its Determinant coeficient value (R^2) and plotted with the XRD data dan FTIR to determine the accuracy of the model.

IV. RESULT AND DISCUSSION

There are six models will be developed by ARIMA. They are ARIMA for and Lanthanum Oxide (0 %, 5 %, 10 %) doped BST FTIR data and Lanthanum Oxide (0 %, 5 %, 10 %) doped BST XRD data. We give two examples plot of Lanthanum Oxide (0 %,) doped BST FTIR data (Figure 1) and Lanthanum Oxide (0 %,) doped BST XRD data (Figure 2). At Figure 1, X is infrared radiation category and y axis is percent of absorption. At Figure 2, X axis is X-Ray spectrum, and y axis is percent of diffraction.

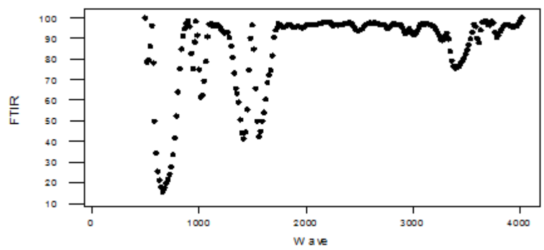

Figure 1. Plot of Lanthanum Oxide (0 %,) doped BST FTIR data

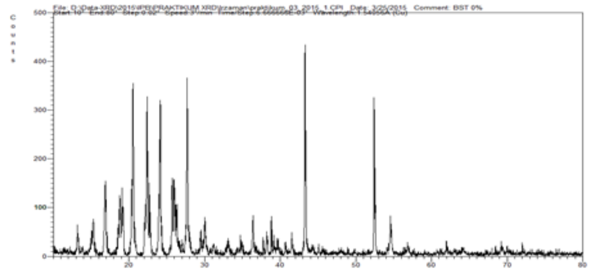

Figure 2. Plot of Lanthanum Oxide (0 %,) doped BST XRD data

At Figure 3 , X is integer number with start value of 1 and y axis is percent of absorption. At Figureb 4, X X is integer number with start value of 1 and y axis is percent of diffraction

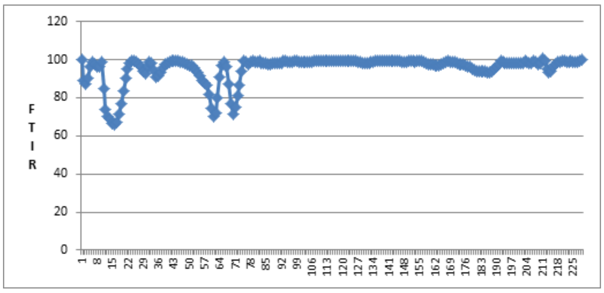

Figure 3. Plot of X is integer number with start value of 1 and y axis is percent of absorption of Lanthanum Oxide (0 %,) doped BST FTIR data

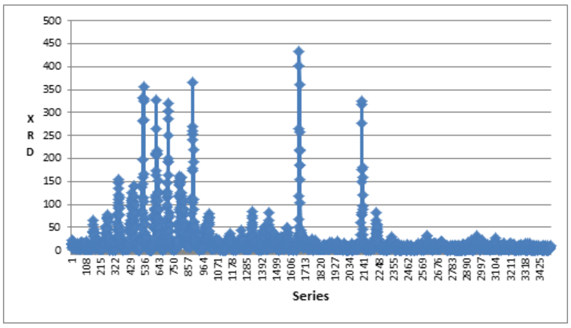

Figure 4. Plot of X is integer number with start value of 1 and y axis is percent of Diffraction of Lanthanum Oxide (0 %,) doped BST XRD data

In the initial step, plotting was done to the Lanthanum Oxide (0%, %, 10 %) doped FTIR and XRD value of BST on non stationary condition in mean. Thus, first differencing was done to the data and replotted. Plot result of the difference value of Lanthanum Oxide (0%, %, 10 %) doped BST FTIR and XRD showed stationary performance. Therefore, develope model was the differencing ARIMA model [59-66].

4.1. ARIMA model on BST FTIR Data

Partial Autocorrelation Function and Autocorrelation Function calculation of Lanthanum Oxide (0% as control) doped BST FTIR data suggest that the suitable model was ARIMA (3,1,3) or less. From the tested model, it turned out tha ARIMA model (2,1,2) was the best model due to its significant parameters of model on alpha 5% with Coefficient of Determinant (R^2) of 93.5%. ARIMA model (2,1,2) was showed at Table 1.

ARIMA model (2,1,2) on Lanthanum Oxide (0 % as control) doped BST FTIR data was $W_i = 1{,}416\ W_{i-1} - 0{,}563\ W_{i-2} + 0.482\ e_{i-1} + 0{,}485\ e_{i-2}$

where,

$W_i = Y_i - Y_{i-1}$ = Difference of Observation FTIR value n=i with FTIR value n = i-1

$W_{i-1} = Y_{i-1} - Y_{i-2}$ = Difference of Observation FTIR value n=i-1 with FTIR value n = i-2

$W_{i-2} = Y_{i-2} - Y_{i-3}$ = Difference of Observation FTIR value n=i-2 with FTIR value n = i-3

Table 1. Significance test of model parameters of ARIMA (2,1,2) on Lanthanum Oxide (0 % as Control) doped FTIR BST data

Model	Lag	Parameters	Standard error	T	Probability
AR	Lag 1	1,416	0,068	20,743	0,000
	Lag 2	-0,563	0,067	-8,387	0,000
Differencing		1			
MA	Lag 1	0,482	0,073	6,626	0,000
	Lag 2	0,485	0,072	6,741	0,000

With high coefficient of Determinant value R^2, 93.5%, it means that Lanthanum Oxide (0%) doped BST FTIR data could be explained 93.5% by the model. This is proved by the plot between Lanthanum Oxide (0% as control) doped BST FTIR estimated data from ARIMA (2,1,2) with Lanthanum Oxide (0% as control) doped BST FTIR data showed in Figure 5. At Figure 5, it could be suggested that the model was good enough due to the estimated data plot pattern was following the data. Fluctuation of Lanthanum Oxide (0%, control) doped BST FTIR data could be well predicted with ARIMA (2,1,2) model.

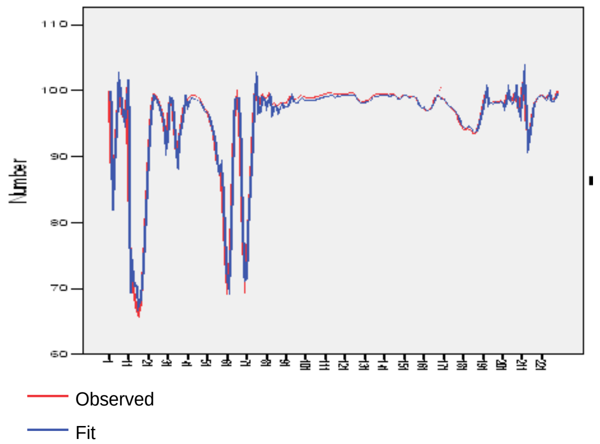

Figure 5. Plot FTIR predicted data from ARIMA (2,1,2) with Lanthanum Oxide (0%, control) doped BST FTIR data

Partial Autocorrelation Function and Autocorrelation Function calculation of Lanthanum Oxide (5%) doped BST FTIR data suggest that the suitable model was ARIMA (3,1,3) or less. Models exploration process were executed with ARIMA (3,1,3), ARIMA (3,1,2), ARIMA (2,1,3), ARIMA (2,1,2), ARIMA (2,1,1) and ARIMA (1,1,2), and the result showed that ARIMA (2,1,1) was the best model due to its significant model parameters with alpha 5%. ARIMA (2,1,1) model on Lanthanum Oxide (5%) doped BST FTIR data was showed in Table 2. This model has Coefficient of Determinant (R^2) of 97 %.

Table 2. Significance test of model parameters of ARIMA (2,1,1) on Lanthanum Oxide (5%) doped BST FTIR data

Model	**Lag**	**Parameters**	**Standard Error**	**T**	**Probability**
AR	Lag 1	0,893	0,088	10,191	0,000
	Lag 2	-0,466	0,078	-5,949	0,000
Differensing		1			
MA	Lag 1	-0,404	0,090	-4,500	0,000

ARIMA model (2,1,1) on Lanthanum Oxide (5 %) doped FTIR BST data was

$W_i = 0{,}893\, W_{i-1} - 0{,}466\, W_{i-2} - 0.404\, e_{i-1}$

where,

$W_i = Y_i - Y_{i-1}$ = Difference of Observation FTIR value n=i with FTIR value n = i-1

$W_{i-1} = Y_{i-1} - Y_{i-2}$ = Difference of Observation FTIR value n=i-1 with FTIR value n = i-2

$W_{i-2} = Y_{i-2} - Y_{i-3}$ = Difference of Observation FTIR value n=i-2 with FTIR value n = i-3

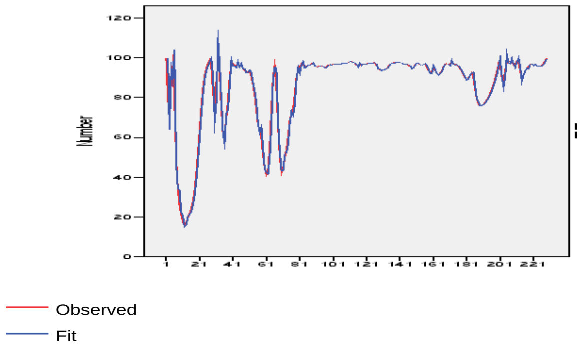

Figure 6. Plot FTIR Predicted data from from ARIMA (2,1,1) with Lanthanum Oxide (5%) doped BST FTIR data

Coefficient of Determinant of ARIMA (2,1,1) model of Lanthanum Oxide (5%) doped BST FTIR, which was 97%, showed that the ARIMA (2,1,1) model was very good. It means the ARIMA (2,1,1) could explain 97% of Lanthanum Oxide (5%) doped BST FTIR data. It also showed in the plot between Lanthanum Oxide (5%) doped BST FTIR estimated data from ARIMA (2,1,1) with its FTIR data on the Figure 6. Figure 6, that the model was good enough since the plot pattern of the predicted data was following the data pattern. Fluctuation of Lanthanum Oxide (5%) doped BST FTIR data could be well predicted with ARIMA (2,1,1) model.

With the same method, Partial Autocorrelation Function and Autocorrelation Function calculation of Lanthanum Oxide (10%) doped BST FTIR data suggest that the suitable model was ARIMA (3,1,3) or less. Models exploration process were executed with ARIMA (3,1,3), ARIMA (3,1,2), ARIMA (2,1,3), and ARIMA (2,1,2), and the result showed that ARIMA (2,1,2) was the best model due to its significant model parameters with alpha 5%. ARIMA (2,1,2) model on Lanthanum Oxide (10%) doped BST FTIR data was showed in Table 3. This model has Coefficient of Determinant (R^2) of 98%.

Table 3. Significance test of model parameters of ARIMA (2,1,2) on Lanthanum Oxide (10 %) doped FTIR BST data.

Model	Lag	Parameters	Standard Error	T	Probability
AR	Lag 1	1.251	0.118	10,571	0,000
	Lag 2	-0,588	0,075	-7,944	0,000
Differensing		1			
MA	Lag 1	-0,457	0,140	-3,258	0,001
	Lag 2	0,416	0,136	3,053	0,003

ARIMA model (2,1,2) on Lanthanum Oxide (10 %) doped FTIR BST data was

$$W_i = 1{,}251\ W_{i-1} - 0{,}588\ W_{i-2} - 0.457\ e_{i-1} + 0{,}416\ e_{i-2}$$

where,

$W_i = Y_i - Y_{i-1}$ = Difference of Observation FTIR value n=i with FTIR value n = i-1

$W_{i-1} = Y_{i-1} - Y_{i-2}$ = Difference of Observation FTIR value n=i-1 with FTIR value n = i-2

$W_{i-2} = Y_{i-2} - Y_{i-3}$ = Difference of Observation FTIR value n=i-2 with FTIR value n = i-3

ARIMA (2,1,2) model of Lanthanum Oxide (10%) doped BST FTIR, with Coefficient of Determinant (R^2) of 98%, showed that the model was very good for studying the Lanthanum Oxide (10 %) doped BST FTIR since there are 98% of Lanthanum Oxide (10%) doped BST FTIR data could be explained by the model. It also showed in the plot between Lanthanum Oxide (10%) doped BST FTIR estimated data from ARIMA (2,1,2) with its FTIR data on the Figure 7. Figure 7, that the model was good enough since the plot pattern of the predicted data was following the data pattern. Fluctuation of Lanthanum Oxide (10%) doped BST FTIR data could be well predicted with ARIMA (2,1,2) model.

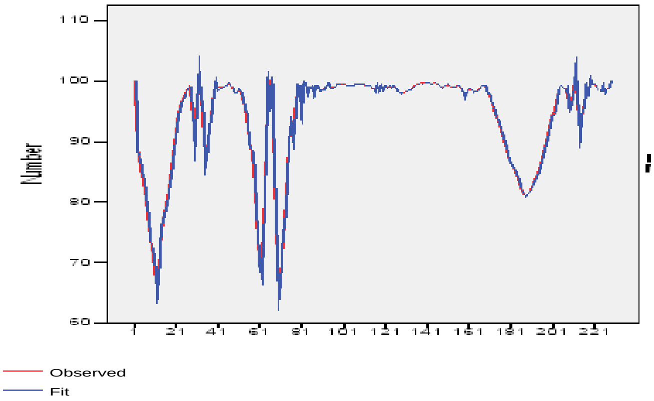

Figure 7. Plot FTIR predicted data from ARIMA (2,1,2) with Lanthanum Oxide (10%) doped BST FTIR data

From the aforementioned explanation, Lanthanum Oxide (0%, 5%, 10%) doped BST FTIR could be well explained by the models ARIMA (2,1,2), ARIMA (2,1,1), and ARIMA (2,1,2) due to its above 95% coefficient of Determinant value.

4.2. ARIMA model on BST XRD data

From the PACF and ACF plot of Lanthanum Oxide (0 %, control) doped BST XRD data, it was suggested that the suitable model was ARIMA (3,1,3) or less. ARIMA (3,1,3) model of Lanthanum Oxide (0%, control) doped BST XRD data had parameters model of ARIMA significant on alpha 5%. Thus, the selected model was ARIMA (3,1,3). ARIMA (3,1,3) model result on Lanthanum Oxide (0%) doped BST XRD data was showed in Table 4. The model had coefficient of Determinant (R^2) = 88% which there were 88% of Lanthanum Oxide (0 %) doped BST XRD data could be explained by the model.

Table 4. Significance test of model parameters of ARIMA (3,1,3) on Lanthanum Oxide (0%) doped XRD BST data

Model	Lag	Parameters	Standard Error	T	Probability
AR	Lag 1	-0,965	0,081	-11,871	0,000
	Lag 2	-0,531	0,080	-6,625	0,000
	Lag 3	-0,506	0,057	-8,925	0,000
Differensing		1			
MA	Lag 1	-1,049	0,078	-13,426	0,000
	Lag 2	-0,771	0,078	-9,887	0,000
	Lag 3	-0,578	0,047	-12,230	0,000

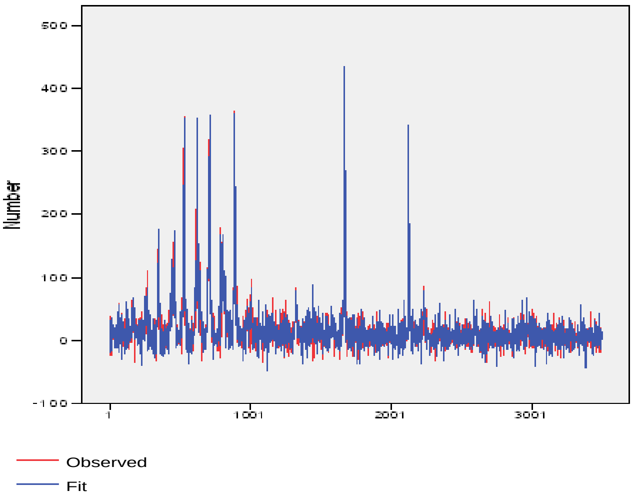

Figure 8. Plot XRD Predicted data from ARIMA (3,1,3) with Lanthanum Oxide (0%, control) BST XRD data

ARIMA model (3,1,3) on Lanthanum Oxide (0%) doped BST XRD data was

Wi= -0,965 Wi-1 -0,531 Wi-2 - 0,506 Wi-3 - 1,049 ei-1 - 0,771 ei-2- 0,578 ei-3

where,

Wi =Yi -Yi-1 = Difference of Observation FTIR value n=i with FTIR value n = i-1

Wi-1 =Yi-1 -Yi-2 = Difference of Observation FTIR value n=i-1 with FTIR value n = i-2

Wi-2 =Yi-2 -Yi-3 = Difference of Observation FTIR value n=i-2 with FTIR value n = i-3

Wi-3 =Yi-3 -Yi-4 = Difference of Observation FTIR value n=i-3 with FTIR value n = i-4

Plot between the Lanthanum Oxide (0%) doped BST XRD predicted data from ARIMA (3,1,3) with the Lanthanum Oxide (0%) doped BST XRD data was shown in Figure 8. In Figure 8, it could be suggested, ARIMA (3,1,3) for Lanthanum Oxide (0 %, control) doped BST XRD data was good enough due to the predicted data plot pattern was following the data pattern.

ARIMA (3,1,3) model also the best model for Lanthanum Oxide (5%) doped BST XRD data. It was due to the PACF and ACF model analysis that suggested the ARIMA (3,1,3) or less, since model parameters of ARIMA (3,1,3) have significancy of 5%. The ARIMA (3,1,3) model result on Lanthanum Oxide (5%) doped BST XRD data was shown in the Table 5. This model had coefficient of Determinant (R^2) = 88%, which means there are 88% of Lanthanum Oxide (5%) doped BST XRD data that could be explainded by model.

Table 5. Significance test of model parameters ARIMA (3,1,3) on Lanthanum Oxide (5%)doped XRD BST data

Model	Lag	Parameters	Standard Error	T	Probability
AR	Lag 1	0,534	0,052	10,359	0,000
	Lag 2	0,859	0,020	43,747	0,000
	Lag 3	-0,497	0,045	-11,136	0,000
Differensing		1			
MA	Lag 1	0,521	0,056	9,313	0,000
	Lag 2	0,787	0,028	28,054	0,000
	Lag 3	-0,312	0,050	-6,211	0,000

ARIMA model (3,1,3) on Lanthanum Oxide (5%) doped BST XRD data was

$W_i = 0{,}534\ W_{i-1} + 0{,}859\ W_{i-2} - 0{,}497\ W_{i-3} + 0{,}521\ e_{i-1} + 0{,}787\ e_{i-2} - 0{,}312\ e_{i-3}$

where,

$W_i = Y_i - Y_{i-1}$ = Difference of Observation FTIR value n=i with FTIR value n = i-1

$W_{i-1} = Y_{i-1} - Y_{i-2}$ = Difference of Observation FTIR value n=i-1 with FTIR value n = i-2

$W_{i-2} = Y_{i-2} - Y_{i-3}$ = Difference of Observation FTIR value n=i-2 with FTIR value n = i-3

$W_{i-3} = Y_{i-3} - Y_{i-4}$ = Difference of Observation FTIR value n=i-3 with FTIR value n = i-4

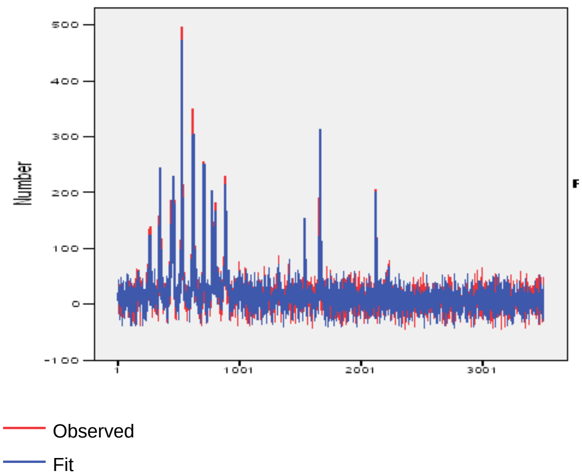

Figure 9. Plot XRD Predicted Data from from ARIMA (3,1,3) with Lanthanum Oxide (5%) doped BST XRD data

Plot between the Lanthanum Oxide (5%) doped BST XRD predicted data from ARIMA (3,1,3) with the Lanthanum Oxide (5%) doped BST XRD was shown in Figure 9. In Figure 9, it could be suggested that ARIMA (3,1,3) for Lanthanum Oxide (5 %) doped BST XRD data was good enough due to the predicted data plot pattern was following the data pattern.

On the Lanthanum Oxide (10 %) doped BST XRD data, it was suggested that the best model was ARIMA (3,1,2). The model parametes was shown in the Table 6. The model had coefficient of Determinant (R^2) = 88% which means there were 88% of Lanthanum Oxide (10%) doped BST XRD data could be explained by the model.

Table 6. Significance test of model parameters of ARIMA (3,1,2) on Lanthanum Oxide (10%) XRD BST data

Model	**Lag**	**Parameters**	**Standard Error**	**T**	**Probability**
AR	Lag 1	0,336	0,021	16,158	0,000
	Lag 2	0,848	0,013	62,599	0,000
	Lag 3	-0,377	0,016	-23,692	0,000
Differensing		1			
MA	Lag 1	0,138	0,017	8,036	0,000
	Lag 2	0,857	0,017	50,535	0,000

ARIMA model (3,1,2) on Lanthanum Oxide (10 %) doped BST XRD data was

Wi= 0,336 Wi-1 +0,848 Wi-2 - 0,377 Wi-3 + 0,138 ei-1 + 0,857 ei-2

where,

Wi =Yi -Yi-1 = Difference of Observation FTIR value n=i with FTIR value n = i-1

Wi-1 =Yi-1 -Yi-2 = Difference of Observation FTIR value n=i-1 with FTIR value n = i-2

Wi-2 =Yi-2 -Yi-3 = Difference of Observation FTIR value n=i-2 with FTIR value n = i-3

Wi-3 =Yi-3 -Yi-4 = Difference of Observation FTIR value n=i-3 with FTIR value n = i-4

Plot between the Lanthanum Oxide (10%) doped BST XRD predicted data from ARIMA (3,1,2) with the Lanthanum Oxide (10 %) doped BST XRD data was shown in Figure 10. In Figure 10, it could be said that ARIMA (3,1,2) for Lanthanum Oxide (10 %) doped BST XRD data was good enough due to the predicted data plot pattern was following the data pattern.

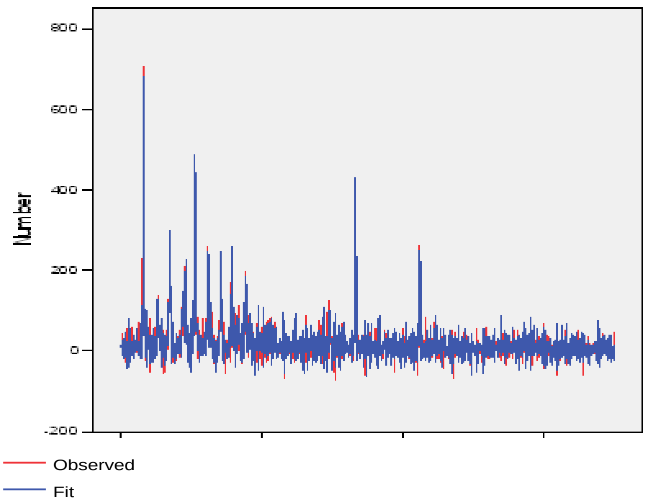

Figure 10. Plot XRD Predicted data dfrom ARIMA (3,1,2) with Lanthanum Oxide (10 %)doped BST XRD data.

From the aforementioned explanation, Lanthanum Oxide (0%, 5%, 10%) doped BST XRD could be well explained by the model ARIMA (3,1,3) and ARIMA (3,1,2) due to its has above 88% coefficient of Determinant value.

4.3. Effect of Lanthanum Oxide enclosure on the FTIR and XRD of BST

To calculate the effect of the Lanthanum Oxide doped the BST FTIR and BST XRD, F Test was done, then followed by T test. The mean value of Lanthanum Oxide of 0% (control), 5%, and 10% doped BST FTIR were 95.6092, 85.8572, 93.7853, respectively. Variance analysis result showed that percentage of Lanthanum Oxide doped BST FTIR affected the BST FTIR value. This was proved from the F test on the Table 7, which showed significant difference.

It is suspected that the addition of lanthanum oxide into the BST, infrared ray spectra capable of vibrating the La-O group bond in the BST compound (capable of vibrating very significantly).

Table 7. Variance Analysis Effect of Lanthanum Oxide to the BST FTIR

Source	Sum of Squares	Degree of freedom	Sum of Mean Squares	F	Probability
Lanthanum Oxide	12311,128	2	6155,564	37,641	,000
Error	111856,855	684	163,533		
Total	124167,983	686			

Meanwhile, mean value Lanthanum Oxide of 0% (control), 5%, and 10% doped BST XRD were 17.3276; 17.6975; 18.8966; respectively. Variance analysis result showed that percentage of Lanthanum Oxide doped to BST XRD did not affect the BST XRD value. This was proved from the F test on the Table 8, which showed not significant difference. It is suspected that the addition of lanthanum oxide into the BST, the x-ray spectral does not move the angle nor increase the intensity of the peak of the diffraction field is not large (shifts the angle and raises the peak intensity of the diffraction field is not significant).

Tabel 8. Analisis Ragam Pengaruh Lantanum Oksida terhadap XRD BST

Source	**Sum of Squares**	**Degree of freedom**	**Sum of Mean Squares**	**F**	**Sig.**
Lanthanum Oxide	4416,746	2	2208,373	1,583	0,205
Error	14645643,976	10500	1394,823		
Total	14650060,722	10502			

V. CONCLUSION

- ✓ First Differencing Model on ARIMA with order AR 2 and Order MA(2) or less, was very good to explain Lanthanum Oxide (0%, 5%, 10%) doped BST FTIR data.
- ✓ First Differencing Model on ARIMA with order AR 3 and Order MA(3) or less, was very good to explain Lanthanum Oxide (0%, 5%, 10%) doped BST XRD data.
- ✓ Accuracy of ARIMA model to explain Lanthanum Oxide (0%, 5%, 10%) doped BST FTIR data was better than to explain Lanthanum Oxide (0%, 5%, 10%) doped BST XRD data (more parsimony) and also had higher coefficient of Determinant.
- ✓ ARIMA (2,1,2) model Lanthanum Oxide (0%) deped BST FTIR data was Wi= 1,416 Wi-1 -0,563 Wi-2 +0.482 ei-1 + 0,485 ei-2. ARIMA (2,1,1) model on Lanthanum Oxide (5%) doped BST FTIR data was Wi= 0,893 Wi-1 -0,466 Wi-2 - 0.404 ei-1. ARIMA (2,1,2) model on Lanthanum Oxide (10%) doped BST FTIR data was Wi= 1,251 Wi-1 -0,588 Wi-2 - 0.457 ei-1 + 0,416 ei-2.
- ✓ ARIMA (3,1,3) model on Lanthanum Oxide (0%) doped BST XRD data was Wi= -0,965 Wi-1 -0,531 Wi-2 - 0,506 Wi-3 - 1,049 ei-1 - 0,771 ei-2- 0,578 ei-. ARIMA (3,1,3) model Lanthanum Oxide (5%) doped BST XRD data was Wi= 0,534 Wi-1 +0,859 Wi-2 - 0,497 Wi-3 + 0,521 ei-1 + 0,787 ei-2 - 0,312 ei. ARIMA (3,1,2) model on Lanthanum Oxide (10%) doped BST XRD data was Wi= 0,336 Wi-1 +0,848 Wi-2 - 0,377 Wi-3 + 0,138 ei-1 + 0,857 ei-2.
- ✓ Mean value of of Lanthanum Oxide (0%, 5% and 10%) doped BST FTIR was different for each, but was not different with the BST XRD value.

VI. REFERENCES

[1]. Jian-Gong C, Tang J, Chu J, Zhang A."Pyroelectric properties in sol–gel derived barium strontium titanate thin films using a highly diluted precursor solution," Applied Physics Letter, Vol. 77, p. 1035-1037, 2000.

[2]. Wenhui Ma dan L. Eric Cross. "Flexoelectric polarization of barium strontium titanate in the paraelectric state,"Applied Physics Letter,Vol. 81, p. 1, 2002.

[3]. Padmini P, Taylor T R, Lefevre M J, Nagra A S, York R A, Speck J S. "Realization of high tunability strontium titanate thin films by rf magnetron sputtering," Applied Physics Letter, Vol. 75, 3186-3188, 1999.

[4]. Frank N, Christian V, JakobsenH."MEMS-Based Uncooled Infrared Bolometer Arrays – A Review," Proceeding of SPIE, Vol. 6836, 1-15, 2013.

[5]. Zhao Y, Mao M, Horowitz R, Majumdar A, Varesi J, Norton P, Kitching J. "Optomechanical Uncooled Infrared Imaging System: Design, Microfabrication, and Performance," Journal Of Microelectromechanical Systems, Vol. 11, 136-146, 2002.

[6]. Polotai A V, Yang G, Dickey E C, Clive A. Randall C A. "Utilization of Multiple-Stage Sintering to Control Ni Electrode," Journal of the American Ceramic Societ, Vol. 90, 3811-3817,2007.

[7]. Opitz M R, Albertsen K, Beeson J J, Hennings D F, Routbort J L, Randall C A. "Kinetic Process of Reoxidation of Base Metal Technology," Journal of the American Ceramic Society, Vol. 86, 1879-1884,2003.

[8]. Ali T, Maria J, Ayguavives F, Jin Z, Stauf G T, Angus I."Tunable Barium Strontium Titanate Thin Film," IEEE Microwave And Wireless Components Letters,Vol. 12, 3-5, 2012.

[9]. Clemens B M."Solid-state reaction and structure in compositionally modulated zirconiumnickel and titanium-nickel films," Physical Review 8, Vol. 33,7615-7623, 1986.

[10]. Han S J, Jang T H, Kim Y B, Park B G, Park J H, Jeong Y H. "Magnetism in Mn-doped ZnO bulk samples prepared by solid state reaction," Applied Physics Letter. Vol. 83, 2003.

[11]. Jin B J, Im S, Lee S Y."Violet and UV luminescence emitted from ZnO thin films grown on sapphire by pulsed laser deposition," Thin Solid Films, Vol. 366, 107-110,2007.

[12]. Kaidashev E M, Lorenz M, Wenckstern H V, Rahm A, Semmelhack H C, Han K H, Benndorf G, Bundesmann C, Hochmuth H, Grundmann M."High electron mobility of epitaxial ZnO thin films on c-plane sapphire grown by multistep pulsed-laser deposition," Applied Physics Letter. Vol.82, 3901-3903, 2003.

[13]. Ma C, Dou A, Chen L, Li Y, Tan X, Dong P, Zhang J,Zheng L, Zhang P."A new nondestructive instrument for bulk residual stress measurement using tungsten Kα1 X-ray,"Review Of Scientific Instruments, Vol. 87, pp. 1-7, 2016.

[14]. Hou Y, Ji X, Zou L, Liu S, Su X."Performance of cement stabilized crushed brick aggregates in asphalt pavement base and subbase applications," Road Materials and Pavement Design pp. 1-16,2015.

[15]. Dubey S, Gubrele D, Rao R M. "Standardization of Yogaamruto Rasa by Using Modern Analysis Techniques," Vol. 4, pp. 27-23, 2016.

[16]. Pawan R, Shalini P, Sridurga Ch. "Analytical Study of Panchshara Rasa Through XRD, SEM, EDX, and ZP," International Journal of Ayurveda and Pharma Research , Vol. 4, pp. 35-40, 2016.

[17]. Erinosho T O, Collins D M, Wilkinson A J,Todd R I, Dunne F P E."Assessment of X-ray Diffraction and Crystal Plasticity Lattice Strain Under Biaxial Loading," International Journal of Plasticity, pp. 1-29, 2016.

[18]. Yusuf N Y, Masdar M S, Isahak W N R W, Nordin D, Husaini T, Majlan E H, Rejab S A M, Chew C L."Ionic liquid impregated activated carbon for biohydrogen purification in an adsorption unit," IOP Conference Series: Materials Science and Engineering, pp. 1-12, 2016.

[19]. Karami F, Khanmohammadi, Garmarudi."ATR-FTIR spectroscopy and chemometrics application for analytical and kinetics characterization of adsorption of 1-butyl mercaptan (1-butanethiol) on nickel coated carbon nanofibers (CNFS),"Bulgarian Chemical Communications,Vol. 48, pp. 51-56, 2016.

[20]. Jiang X, Li S, Xiang G, Li Q, Fan L, He L, Gu K. "Determination of the acid values of edible oils via FTIR spectroscopy based on the OAH stretching band,"Food Chemistry,Vol. 212, pp. 585-589, 2016.

[21]. Toon G C, Blavier J, Sung K, Rothman L S, Gordon I E."HITRAN spectroscopy evaluation using solar occulation FTIR spectra," Journal of Quantitative Spectroscopy & Radiative Transfer, Vo. 182,pp. 324-336, 2016.

[22]. Liao J X, Wei X B, Xu Z Q, Wang P."Effect of potassium-doped concentration on structures and dielectric performance of barium-strontium-titanate films," Vacuum, Vol. 107, pp. 291-296, 2014.

[23]. Zuo X H, Deng X Y, Chen Y, Ruan M ,Li W, Liu B, Qu Y, Xu B."A novel method for preparation

of barium strontium titanate nanopowders, " Materials Letters, Vol. 64, pp. 1150-1153, 2010.
[24]. Tubchareon T, Soisuwan S, Ratanathammaphan S, Praserthdam P."Effect of Na-, K-, Mg-, and Ga dopants in A/B-sites on the optical band gap and photoluminescence behavior of [Ba0.5Sr0.5]TiO3 powders," Journal of Luminescence,Vol. 142, pp. 75-80, 2013.
[25]. Liu C, Liu P, Li X, Gao C, Zhu G, Chen X."A simple method to synthesize Ba0.6Sr0.4TiO3 nano-powders through high-energy ball-milling," Powder Technology, Vol. 212, pp.299-302, 2011.
[26]. Challali F, Besland M P,Benzeggouta D, Borderon C, Hugon M C, Salimy S, Saubat J C,Charpentier A, Averty D, Goullet A, Landesman J P."Investigation of BST thin films deposited by RF magnetron sputtering in pure Argon," Thin Solid Films, Vol. 518, pp. 4619-4622, 2010.
[27]. Brankovic G, Brankovic Z , Goes M S, Paiva-Santos C O P, Cilense M, Varela J A, Longo E."Barium strontium titanate powders prepared by spray pyrolysis," Materials Science and Engineering B, Vol. 122, pp. 140-144, 2005.
[28]. Xiaowei Y, Yanwei Z, Tongxiang C, Zhenxing H."Preparation of (Ba,Sr)TiO3@polystrene core-shell nanoparticles by solvent-free surface-initiated atom transfer radical polymerization," Applied Surface Science, Vol. 258, pp. 7365-7371, 2012.
[29]. Mohammadi M R, Derek J. Fray D J."Sol–gel derived nanocrystalline and mesoporous barium strontium titanate prepared at room temperature," Particuology, Vol. 9, pp. 235-242, 2011.
[30]. Norezan I, Yahya A K, Talari M K."Effect of (Ba0.6Sr0.4)TiO3 (BST) Doping on Dielectric Properties of CaCu3Ti4O12 (CCTO)," Journal of Materials Science & Technology,Vol. 28, pp. 1137-1144, 2012.
[31]. Wanga X, Huang R, Zhao Y, Zhao Y, Zhoub H, Jiaa Z."Dielectric and tunable properties of Zr doped BST ceramics prepared by spark plasma sintering,"Journal of Alloys and Compounds, Vol. 533, pp. 25-28, 2012.
[32]. Sohail S, Mistri E A, Khanb A, Banerjee S, Biswas K."Fabrication and performance study of BST/Teflon nanocomposite thin film for low voltage electrowetting devices," Sensors and Actuators A, Vol. 238, pp. 122-132, 2016.
[33]. Liua T, Zhanga H, Wanga F, Shi J, Ci P, Wanga L, Ge S, Wang Q, Chu P K."Three-dimensional supercapacitors composed of Ba0.65Sr0.35TiO3 (BST)/NiSi2/silicon microchannel plates," Materials Science and Engineering B,Vol. 176, pp. 387-392, 2011.
[34]. Jian S, Chang W, Fang T, Ji L, Hsiao Y, Chang Y."Nanomechanical characteristics of BaxSr1−xTiO3 thin films," Materials Science and Engineering B, Vol. 131, pp. 281-284, 2006
[35]. Nur O, Willander M, Israr M Q, Desouky E F G, Salem M A, Hamad A B A , Battisha I K. "Effect of elevated concentrations of strontium and iron on the structural and dielectric characteristics of Ba(1xy)Sr(x)Ti Fe(y)O3 prepared through sol–gel technique," Physica B, Vol. 407, pp. 2697-2704, 2012.
[36]. Yana D, Luob L, Zhang Y, Penga Z, Liua H, Xiao D , Liub T, Laib X, Zhu J."Influence of deposition temperature on microstructure and electrical properties of modified (Ba, Sr)TiO3 ferroelectric thin films,"Ceramics International Vol. 41, pp. 520-525, 2015.
[37]. Rani R, Singh S, Juneja J K, Raina K K, Prakash C."Dielectric properties of Zr substituted BST ceramics," Ceramics International, Vol. 37, pp. 3755-3758, 2011.
[38]. 38Huang J, Liao J, Wang P, Zhang W, Wei X, Xu Z. "Effect of doped concentration on dielectric properties of Mn and Y alternately doped BST films," Surface & Coatings Technology,Vol. 251, pp. 307-312, 2015
[39]. 39Wang S Z, Liao J X, Hu Y M, Gong F, Xu Z Q, Wu M Q."Structures and dielectric performances of Mn/Y alternately doped BST films prepared by a novel preheating process,"

Materials Chemistry and Physics,Vol. 193, pp. 50-56, 2017.

[40]. 40Maensiri S, Nuansing W, Klinkaewnarong J, Laokul P, Khemprasit J."Nanofibers of barium strontium titanate (BST) by sol–gel processing and electrospinning," Journal of Colloid and Interface Science, Vol. 297, pp. 578-583, 2006.

[41]. 41Singh M, YadavaB C., Ranjan A, Kaur M, GuptaS K."Synthesis and characterization of perovskite barium titanate thin film and its application as LPG sensor,"Sensors and Actuators B,Vol. 241, pp. 1170-1178, 2017.

[42]. 42Rai K, RaoKN, Kumar L V, MandalK D."Synthesis and characterization of ultra fine barium calcium titanate, barium strontium titanate and Ba1–2xCaxSrxTiO3 (x = 0.05, 0.10),"Journal of Alloys and Compounds,Vol. 475, pp. 316-320, 2009.

[43]. 43Simões A Z, Moura F, Onofre T B, Ramirez M A, Varela J A, Longo E."Microwave-hydrothermal synthesis of barium strontium titanate nanoparticles," Journal of Alloys and Compounds, Vol. 508, pp. 620-624,2010.

[44]. 44KhollamYB, DeshpandeSB, PotdarHS, BhoraskarSV, SainkarSR, DateSK."Simple oxalate precursor route for the preparation of barium–strontium titanate: Ba1xSrxTiO3 powders," Materials Characterization, Vol. 54, pp. 63-74. 2005.

[45]. 45Dong H, Jian J, Li H, Jin D, Chen J and Cheng J."Improved dielectric tunability of PZT/BST multilayer thin films on Ti Substrate," Journal of Alloys and Compounds, 2017.

[46]. 46Pan Z B, Yao L M , Zhai J W, LiuSH, Yang K, Wang H T, Liu J H."Fast discharge and high energy density of nanocomposite capacitors using Ba0.6Sr0.4TiO3 nanofibers," Ceramics International, 2016.

[47]. 47Philippot G, JensenKMØ, Christensen M, Elissalde C, Maglione M, IversenbBo B, Aymonier C."Coupling in situ synchrotron radiation with ex situ spectroscopy characterizations to study the formation of Ba1–xSrxTiO3 nanoparticles in supercritical fluids," Journal of Supercritical Fluids, Vol. 87, pp. 111-117, 2014.

[48]. 48Liu S, Xue S, Zhang W, Zhai J, Chen G."The influence of crystalline transformation of Ba0.6Sr0.4TiO3 nanofibers/poly (vinylidene fluoride) composites on the energy storage properties by quenched technique," Ceramics International, pp. 1-5, 2014.

[49]. 49Jin Y, Xia N, Gerhardt R A."Enhanced Dielectric Properties of Polymer Matrix Composites with BaTiO3 and MWCNT Hybrid Fillers using Simple Phase Separation," Nano Energy, pp. 1-33, 2016.

[50]. 50Attar A S, Sichani E S , Sharaf S."Structural and dielectric properties of Bi-doped barium strontium titanate nanopowders synthesized by sol–gel method," Journal of Materials Research and Technology, Vol. 216, pp. 1-8, 2016.

[51]. 51Kumari A, Ghosh B D. "Preparation and dielectric properties of polyimide/Ba0.7Sr0.3TiO3 nanocomposite film," Materials Today: Proceedings, Vol. 4, pp. 10479-10483, 2017.

[52]. 52ChenQ, HongR Y."Fabrication and characterization of Ba0.5Sr0.5TiO3-PANI/PS three-phase composites," Ceramics International, pp. 1-36, 2014.

[53]. 53Naeem A, Mahmood A , Iqbal Y , Ullah A , Mahmood T, Humayun M. "Dielectric and impedance spectroscopic studies on (Ba0.5Sr0.5)Mnx(Ti0.95Fe0.05)1xO3 ceramics synthesized by using sol–gel method," Journal of Alloys and Compounds, Vol. 645, pp. 290-296, 2015.

[54]. 54Turkya A O, Rashad M, and Bechelany M."Tailoring Optical and Dielectric Properties of Ba0.5Sr0.5TiO3 Powders Synthesized Using Citrate Precursor Route," Materials Design, pp. 1-22, 2015.

[55]. 55Irzaman, H. Syafutra, E. Rancasa, A. Wahidin Nuayi, Tb. Gamma Nur Rahman, N. Aisyah Nuzulia, I. Supu, Sugianto, F. Tumimomor, Surianty, O. Muzikarno, and Masrur. The Effect of BaSr Ratio on Electrical and Optical

Properties of BaxSr(1-x)TiO3 (x = 0.25; 0.35; 0.45; 0.55) Thin Film Semiconductor. Ferroelectrics. Vol. 445 (1) : 4-17,2013.

[56]. 56M. Nur Aidi. M. Masjkur, Siswadi, S. Pramudito, A. Arif, H. Syafutra, H. Alatas, dan Irzaman. Phase Transformation of Ba0.55Sr0.45TiO3 Tetragonal to Pseudotetragonal Structures and Arima Model for XRD Data. International Journal of Statistic and Application. Vol. 3 (5): 19-187, 2013.

[57]. 57Irzaman, Y. Pebriyanto, E. Rosidah Apipah, I. Noor, A. Alkadri. Characterization of Optical and Structural of Lanthanum Doped LiTaO3 Thin Films. Integrated Ferroelectrics. Vol. 167(1), page 137-145,2015.

[58]. 58Irzaman, Henni Sitompul, Masitoh, Mohammad Misbakhusshudur and Mursyidah. Optical and Structural Properties of Lanthanum Doped Lithium Niobate Thin Films. Ferroelectrics. Vol. 502 (1), page 9-18, 2016.

[59]. 59Liu K., Chen Y. and Zhang X. "An Application of the Seasonal Fractional ARIMA model to the Semiconductor Manufacturing," IFAC PapersOnline, Vol. 50-1, pp. 8097-8102, 2017.

[60]. 60Sen P, Roy M and Pal P."Application of ARIMA for forecasting energy consumption and GHG emission: A case study of an indian pig iron manufacturing organization," Energy, pp. 1031-1038, 2016.

[61]. 61Zafra C, Angel Y and Torres E."ARIMA analysis of the effect of land surface coverage on PM10 concentrations in a high-altitude megacity," Atmospheric Pollution Research, pp. 1-9, 2017.

[62]. 62Yuan C, Liu S and Fang Z."Comparison of China's primary energy consumption forecasting by using ARIMA and GM model," 2016, pp. 384-390. 2016

[63]. 63Jeyasekar A, Raja SVK and Uthra RA."Congestion Avoidance Algorithm Using ARIMA Model-Based RTT in Heterogeneous Wired-Wireless Networks,"Journal of Network and Computer Application, pp. 1-42, 2016.

[64]. 64Oliveira PJ, SteffenJL and CheungP."Parameter Estimation of Seasonal Arima Models for Water Demand FOrecasting using the Harmony Search Algorithm," Procedia Engineering, Vol. 186, pp. 177-185, 2017.

[65]. 65Koutroumanidis T, Ioannou K, ArabatzisGaryfallos. "Predicting fuelwood pricesin Greece with the use of ARIMA models, artificial neural network and hybrid ARIMA-ANN model," Energy Policy, Vol. 37, pp. 3627-3634, 2009

[66]. 66Qin M, Li Z. and Du Z. "Red tide time series forecasting by combining ARIMA," Knowledge-Based Systems, pp. 1-24, 2017.

[67]. 67Box, George; Jenkins, Gwilym (1970). Time Series Analysis: Forecasting and Control. San Francisco: Holden-Day.